American Journal of Life Sciences
2026, Vol. 14, No. 6, pp. 143–153
https://doi.org/10.11648/j.ajls.20261406.11

SciencePG
Science Publishing Group

Research Article

Heterologous Overexpression of *PeNHX3* from *Populus euphratica* Enhances Salt Stress Tolerance in *Arabidopsis thaliana*

Peiyang He*

College of Life Sciences, Fujian Agriculture and Forestry University, Fuzhou, China

Abstract

The NHX-type Na^+/H^+ antiporters are key membrane proteins that maintain intracellular ion homeostasis under salt stress, whereas their functions in the desert tree *Populus euphratica* remain poorly understood. This study aimed to identify the NHX gene family in *P. euphratica* and to screen candidate genes for salt tolerance, and to verify the function of the screened gene through heterologous expression. Genome-wide identification, combined with analyses of gene structure, conserved motifs, physicochemical properties, and promoter cis-elements, yielded six PeNHX genes distributed on five scaffolds, all containing the Na^+/H^+_Exchanger domain; *PeNHX*1–5 clustered with the vacuolar *AtNHX*1–4, and *PeNHX6* clustered with the endosomal *AtNHX*5/6. Under 300 mmol/L NaCl treatment, the expression of these genes in roots, stems, and leaves was quantified by qRT-PCR, and *PeNHX*3 showed the strongest induction among all members, reaching approximately 33-fold of the control level in stems at 12 h. A 35S:: PeNHX3-GFP fusion protein transiently expressed in Nicotiana benthamiana. *PeNHX3*-overexpression *Arabidopsis* lines obtained by the floral dip method exhibited significantly greater primary root length and shoot fresh weight than the wild type under 100 and 150 mmol/L NaCl. These results indicate that *PeNHX3* improves salt tolerance when heterologously expressed and is a promising candidate gene for salt-tolerance breeding of woody plants.

Keywords

Populus euphratica, *PeNHX3*, Salt Stress, Na^+/H^+ Antiporter, Subcellular Localization, Heterologous Overexpression

1. Introduction

Soil salinization constrains approximately 20% of the global arable land and nearly 50% of the irrigated cropland [1]. Salt stress is first manifested as osmotic stress and subsequently turns into ionic stress as Na^+ and Cl^- accumulate in leaves [2], accompanied by oxidative stress and nutrient deficiency [3]. Plants cope with salt stress mainly through osmotic adjustment, ion homeostasis, and antioxidant pathways [4, 5].

Na^+/H^+ antiporters (NHX) drive Na^+ transport across membranes by utilizing the transmembrane electrochemical proton gradient and are key membrane proteins for the maintenance of ion homeostasis [6]. According to their subcellular localization, they can be classified into three types: the vacuolar type (*AtNHX1*, which sequesters cytosolic Na^+ into the vacuole [7]), the endosomal type (*AtNHX*5/6, involved in endosomal pH homeostasis and protein sorting [8]), and the plasma

*Correspondence: Peiyang He (15090921733@163.com)

Received: 6 October 2026; **Accepted:** 26 October 2026; **Published:** 10 November 2026

Copyright: © The Author(s), 2026. Published by Science Publishing Group. This is an **Open Access** article, distributed under the terms of the Creative Commons Attribution 4.0 License (http://creativecommons.org/licenses/by/4.0/), which permits unrestricted use, distribution and reproduction in any medium, provided the original work is properly cited.

membrane type (*SOS1*/*AtNHX7*, which mediates Na^+ efflux [9]). NHX gene families have been identified in wheat [10], Tetragonia tetragonoides [11], and rye [12], and overexpression of *OsNHX1* in rice and *LeNHX2* in tomato has also been shown to enhance salt tolerance [13, 14].

Populus euphratica Oliv. is the only tree species of the Salicaceae naturally distributed in desert regions, and it can survive in nutrient solution containing 450 mmol/L NaCl [15]. Gene families involved in ion transport and ROS scavenging are markedly expanded in its genome [16], and several salt-tolerance genes, including *PeERF1* [17], *PeHINT2* [18], and *PeuDBRH57* [19], have been reported. Ye et al. [20] verified the transport activity of NHX members from *P. euphratica* in yeast, and Wang et al. [21] and Pan et al. [22] clarified the contributions of key residues and transmembrane domain 11, respectively, to PeNHX3-mediated transport. However, the spatiotemporal expression patterns of this family under salt stress and its in vivo functions remain unclear. In this study, we identified the NHX gene family in *P. euphratica* and analyzed its expression patterns, and then subjected *PeNHX3* to subcellular localization and heterologous overexpression analysis.

2. Materials and Methods

2.1. Plant Materials and Salt Stress Treatment

Plantlets of *P. euphratica* and wild-type *Arabidopsis thaliana* (ecotype Col-0) were maintained in our laboratory. The *P. euphratica* plantlets were subcultured on Murashige and Skoog (MS) medium at (24±1) ℃ under a 16-h light/8-h dark photoperiod. Four-week-old plantlets were transferred to 1/2 Hoagland nutrient solution for a 3-day adaptation, after which NaCl was added to a final concentration of 300 mmol/L (set with reference to the report that *P. euphratica* tolerates 450 mmol/L NaCl [15]); nutrient solution without NaCl served as the control. Roots, stems, and leaves were sampled at 0, 12, 24, and 96 h, immediately frozen in liquid nitrogen, and stored at −80 °C. Arabidopsis seeds were surface-sterilized and stratified, sown on 1/2 MS medium containing 0.8% agar (pH 5.8), and grown at 23 ℃ under a 16-h light/8-h dark photoperiod.

2.2. Identification and Bioinformatic Analysis of PeNHX Family Members

NHX family sequences of *P. euphratica* and Arabidopsis were retrieved from NCBI and Phytozome v13. The P. euphratica proteome was searched by BLASTP (Basic Local Alignment Search Tool, protein query) using AtNHX amino acid sequences as queries; homologous sequences with complete open reading frames were retained, and their domains were verified with NCBI Conserved Domain Database (CDD). Chromosomal distribution and gene structure diagrams were drawn with TBtools, conserved motifs were analyzed using MEME Suite 5.5 (the number of motifs was set to 10), physicochemical properties were predicted with ExPASy ProtParam, and subcellular localization was predicted with WoLF PSORT.

2.3. Phylogenetic Analysis

AtNHX sequences were obtained from TAIR. After alignment with ClustalW, a neighbor-joining phylogenetic tree was constructed using MEGA 11 (Bootstrap = 1,000), and a homology heatmap was drawn with TBtools.

2.4. Analysis of Promoter Cis-Elements

The 2,000-bp sequences upstream of the ATG start codon of each gene were extracted, and cis-acting elements were predicted with PlantCARE and visualized with TBtools.

2.5. RNA Extraction and qRT-PCR Analysis

Total RNA was extracted with the Trizol reagent, and its concentration and purity were determined with a NanoDrop-2000 spectrophotometer prior to reverse transcription into complementary DNA (cDNA). The quantitative reverse transcription PCR (qRT-PCR) reaction (20 μL) contained 10.0μL of 2×SYBR® Premix Ex Taq™, 0.4 μL of each forward and reverse primer (10 μmol/L), 0.4 μL of ROX Reference Dye (50×), 2.0 μL of cDNA template, and 6.8 μL of RNase-free ddH_2O. The amplification program was 95 ℃ for 30 s, followed by 40 cycles of 95 ℃ for 5 s and 60 ℃ for 31 s. Actin of P. euphratica was used as the internal reference, and relative expression levels were calculated with the $2^{-\Delta\Delta Ct}$ method [23], with three technical replicates per time point. Primers were designed with Primer3 and verified by BLAST.

2.6. Subcellular Localization of the PeNHX3 Protein

The coding sequence of *PeNHX3* (without the stop codon) was amplified by polymerase chain reaction (PCR) and cloned into pBI121-GFP (green fluorescent protein) by homologous recombination to generate the 35S:: PeNHX3-GFP construct, which was then introduced into *Agrobacterium tumefaciens* GV3101. Bacterial cells were resuspended in infiltration buffer (10 mmol/L MES, 10 mmol/L $MgCl_2$, and 150 μmol/L acetosyringone, pH 5.6) to an optical density at 600 nm (OD_{600}) of ≈0.8 and infiltrated into leaves of *Nicotiana benthamiana*. Co-localization of GFP fluorescence with an mCherry membrane marker was observed 48–60 h later [24]. Because GFP was fused to the C terminus in this construct, the possible influence of the tag on targeting must be considered when interpreting the results [25].

2.7. Generation and Identification of *PeNHX3*-Overexpression Arabidopsis

Wild-type Arabidopsis was transformed by the floral dip method [26]. T_1 seeds were screened on 1/2 MS medium containing 50 mg/L kanamycin, and resistant seedlings were identified by PCR with pBI121-F and PeNHX3-R primers. The transcript levels of *PeNHX3* in each line were determined by qRT-PCR, and homozygous lines were obtained by selfing through the T_2 and T_3 generations.

2.8. Salt Tolerance Analysis of Overexpression Lines Under Salt Stress

Seeds of the wild type and T_3 homozygous overexpression (OE) lines (OE-8, OE-10, and OE-12) were surface-sterilized and stratified, spotted onto 1/2 MS medium containing 0, 50, 100, or 150 mmol/L NaCl, and grown vertically for 10 d. Primary root length was measured and shoot fresh weight was determined, with three replicates per treatment.

2.9. Statistical Analysis

One-way analysis of variance was performed with SPSS 26.0, and differences among treatments were tested for significance by Duncan's multiple range test ($P<0.05$).

3. Results

3.1. Identification and Physicochemical Properties of PeNHX Family Members

A search of the *P. euphratica* genome with AtNHX protein sequences yielded six PeNHX genes (Tables 1 and 2). The encoded proteins are 528–555 amino acids in length, with molecular weights of 58.37–61.36 kDa and grand average of hydropathy (GRAVY) values of 0.46–0.53, indicating hydrophobic membrane proteins; their isoelectric points all exceed 8.0 except that of PeNHX6 (5.48). All six proteins contain the Na^+/H^+_Exchanger domain and belong to the cation/proton antiporter 1 (CPA1) superfamily. PeNHX6 contains the largest number of acidic residues (41) and the smallest number of basic residues (27).

Table 1. *Basic information of the PeNHX gene family in Populus euphratica.*

Gene name	Gene ID	Scaffold	Gene length (bp)	CDS length (bp)	Protein length (aa)
PeNHX1	105132046	GWHAAYU0000014.1	6,122	1,587	528
PeNHX2	105131313	GWHAAYU0000006.1	6,013	1,635	544
PeNHX3	105124949	GWHAAYU0000007.1	5,990	1,638	545
PeNHX4	105114582	GWHAAYU0000010.1	4,653	1,611	536
PeNHX5	105124990	GWHAAYU0000007.1	4,307	1,668	555
PeNHX6	105136432	GWHAAYU0000013.1	8,492	1,602	533

Table 2. *Physicochemical properties and predicted subcellular localization of PeNHX proteins.*

Gene name	MW (kDa)	pI	GRAVY	Instability index	Main WoLF PSORT signals	Main prediction
PeNHX1	58.68	8.95	0.510	36.53	plas: 11, E.R.: 2, vacu: 1	Plasma membrane
PeNHX2	60.61	8.39	0.460	37.90	plas: 7, vacu: 4, E.R.: 2, mito: 1	Plasma membrane/vacuole
PeNHX3	60.29	8.13	0.530	39.25	plas: 7, vacu: 4, golg: 2, mito: 1	Plasma membrane/vacuole
PeNHX4	59.55	8.76	0.504	43.97	plas: 6, vacu: 4, E.R.: 2, mito: 1, extr: 1	Plasma membrane/vacuole
PeNHX5	61.36	8.80	0.505	34.12	plas: 9, vacu: 2, nucl: 1, E.R.: 1	Plasma membrane
PeNHX6	58.37	5.48	0.478	38.50	plas: 12, nucl: 1, vacu: 1	Plasma membrane

3.2. Genomic Distribution and Gene Structure of PeNHXs

The six PeNHX genes are unevenly distributed on five scaffolds, with *PeNHX3* and *PeNHX5* adjacent to each other on GWHAAYU0000007.1. All are single-copy genes, and no tandem duplication was observed (Figure 1). Gene structure analysis (Figure 2) showed that *PeNHX1* and *PeNHX2* contain more exons, whereas *PeNHX*3–5 contain fewer; *PeNHX6* has the longest gene (8,492 bp), with markedly extended introns.

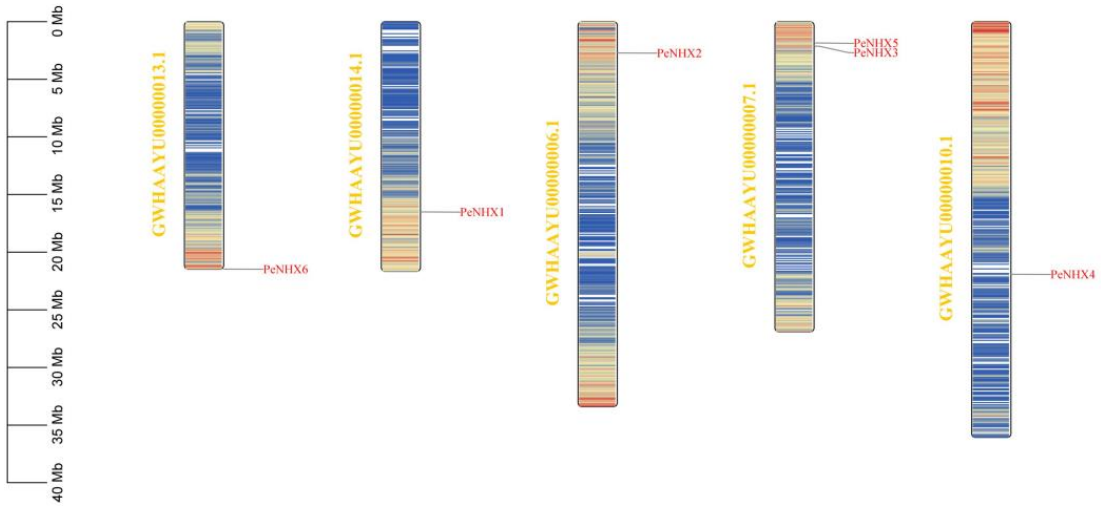


Figure 1. *Distribution of PeNHX genes on the P. euphratica genome.*

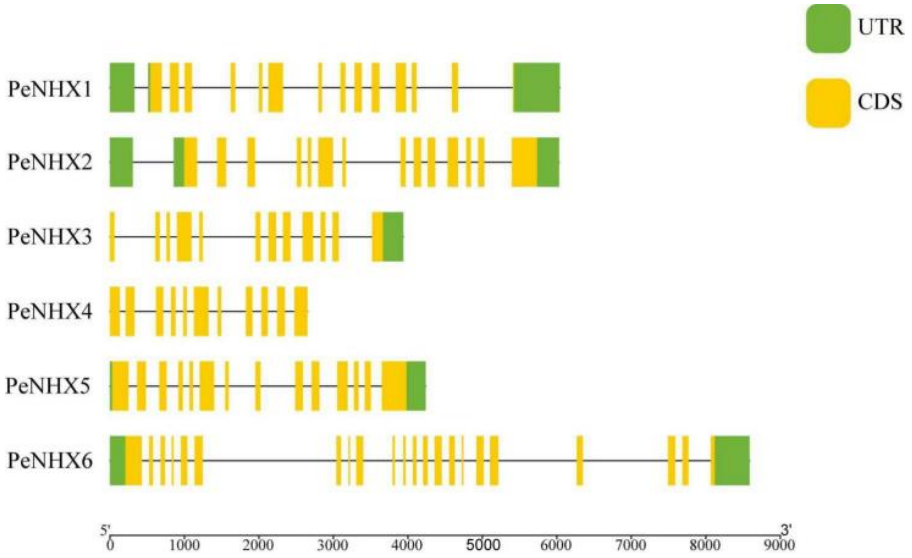


Figure 2. *Gene structure analysis of PeNHXs.*

3.3. Conserved Domains and Motifs of PeNHX Proteins

All six proteins contain the Na^+/H^+_Exchanger domain extending from the N terminus to the central transmembrane region (Figure 3). The core motif FFIYLLPPI is fully conserved in PeNHX1–4; PeNHX5 retains only YLLPPI, and this region is completely divergent in PeNHX6. MEME analysis identified ten conserved motifs (Figure 4): PeNHX1–4 all contain Motifs 1–7; PeNHX5 lacks Motifs 4 and 7 and harbors the unique C-terminal Motif 8; PeNHX6 lacks Motifs 1, 3, 5, and 7 and contains the unique Motifs 9 and 10.

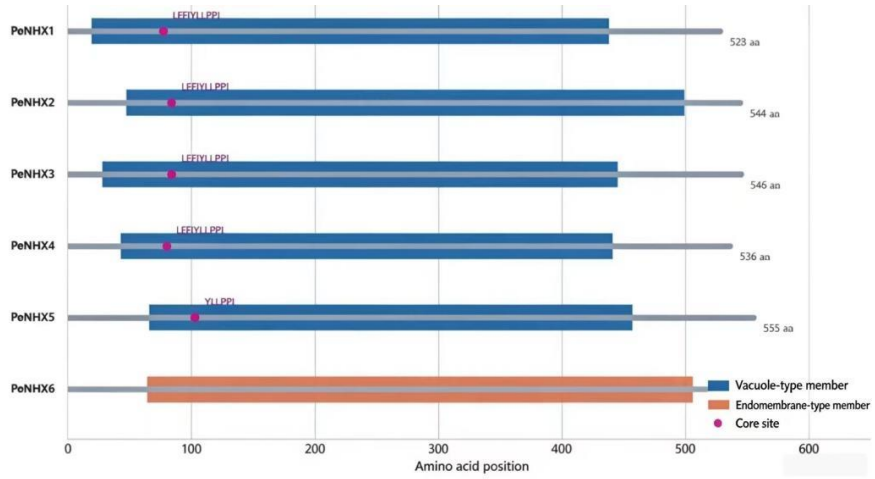


Figure 3. *Conserved domain analysis of PeNHX proteins.*

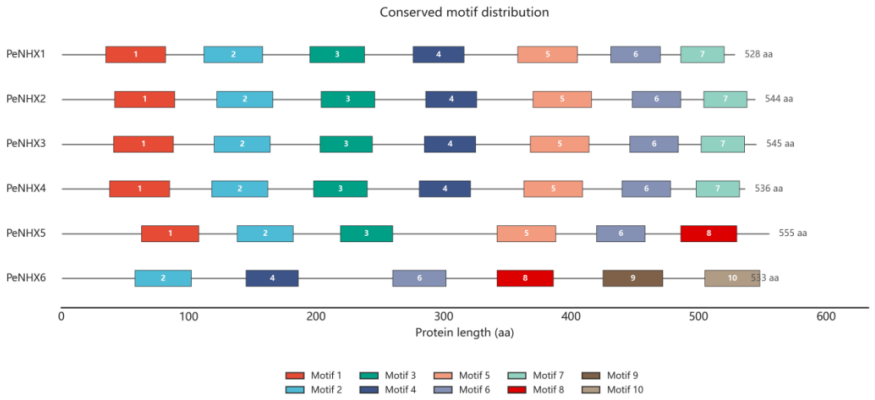


Figure 4. *Distribution of conserved motifs in PeNHX proteins.*

3.4. Phylogenetic Analysis of PeNHXs

The neighbor-joining tree (Figure 5) shows that *PeNHX*1–5 cluster with the vacuolar *AtNHX*1–4, among which *PeNHX3* shares the highest identity with *AtNHX3* (approximately 65%); *PeNHX6* clusters with the endosomal *AtNHX5/6*. The homology heatmap (Figure 6) shows that the identities of *PeNHX*1–5 with *AtNHX*1–4 exceed 60%, whereas that of PeNHX6 with *AtNHX*5/6 is only approximately 40%.

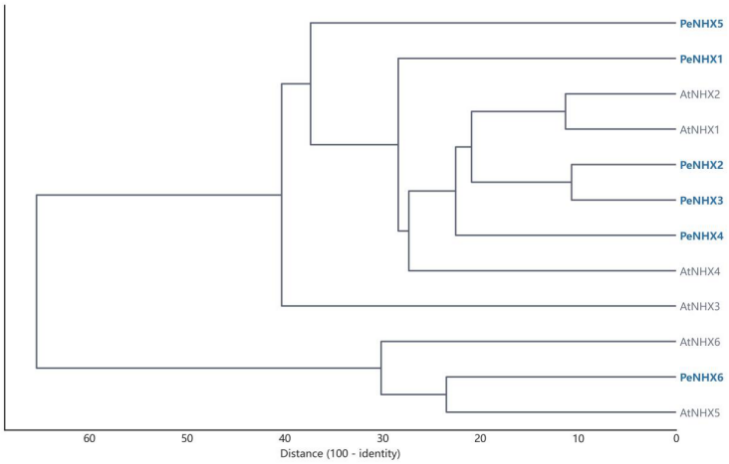


Figure 5. *Phylogenetic tree of PeNHXs and AtNHXs.*

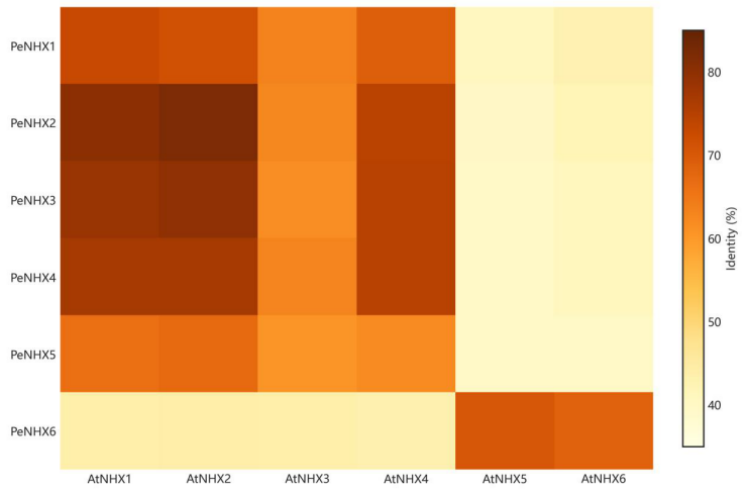


Figure 6. *Identity analysis between PeNHXs and AtNHXs.*

3.5. Prediction of PeNHX Subcellular Localization

WoLF PSORT predicted the plasma membrane as the principal localization signal for all six proteins (Figure 7); *PeNHX6* received the highest score (12) and showed almost no vacuolar signal.

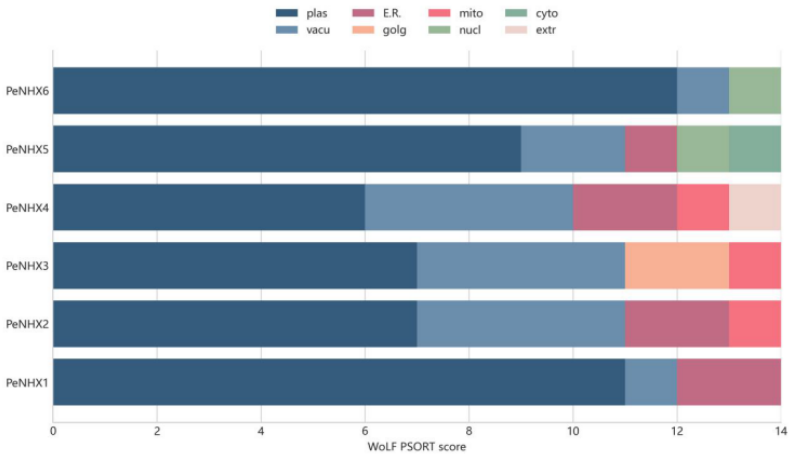


Figure 7. Predicted subcellular localization of PeNHX proteins.

3.6. Cis-Elements in PeNHX Promoters

A total of nine core cis-acting elements were detected within the 2,000-bp regions upstream of the six genes, belonging to three categories: stress response, light response, and hormone response (Figure 8). Box 4 is present in all six promoters and is most abundant in the *PeNHX2* promoter; abscisic acid (ABA)-responsive element (ABRE) is detected in every member; MeJA-responsive elements occur in *PeNHX2* and *PeNHX*4–6. MYB binding site (MBS) is unique to *PeNHX4*; *PeNHX6* contains low-temperature-responsive element (LTR); and *PeNHX1* and *PeNHX3* contain anaerobic-responsive element (ARE).

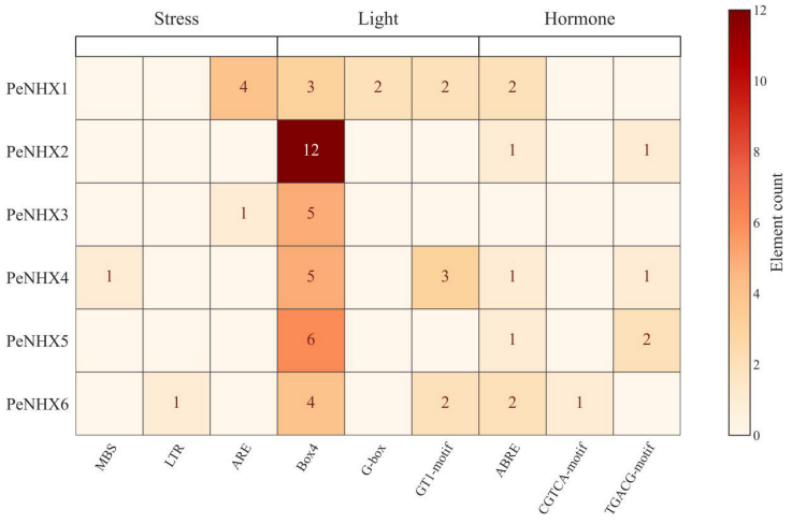


Figure 8. *Cis-acting elements in PeNHX gene promoters.*

3.7. Expression Patterns of PeNHXs Under Salt Stress

After treatment with 300 mmol/L NaCl, the responses of individual members showed pronounced tissue specificity (Figure 9). *PeNHX3* was the most strongly induced, reaching approximately 7-fold in roots at 12 h and approximately 33-fold in stems at 12 h, where induction remained above 12-fold and 9-fold at 24 h and 96 h, respectively; in leaves, *PeNHX3* was induced approximately 4.5-fold at 12 h and then declined to about 3-fold. *PeNHX5* ranked second (approximately 12-fold in stems at 96 h); *PeNHX1* and *PeNHX2* showed moderate induction (1.8–3.5-fold); *PeNHX6* was only mildly up-regulated (1.2–1.7-fold); and *PeNHX4* was down-regulated in all three tissues. *PeNHX3* was therefore selected for functional validation.

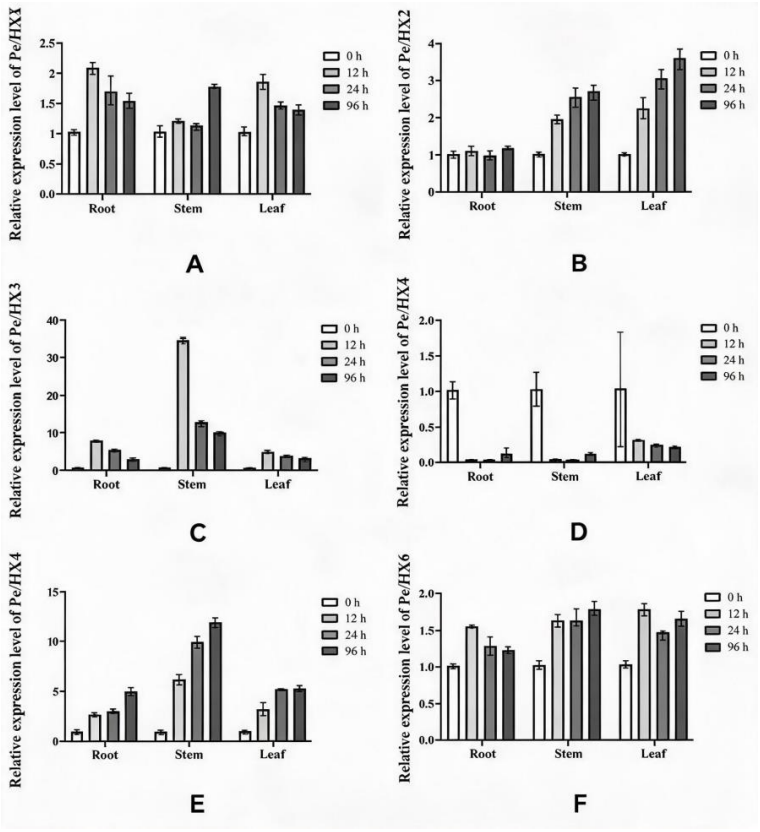


Figure 9. *Relative expression levels of PeNHXs in roots, stems, and leaves of P. euphratica under salt stress.*

3.8. Subcellular Localization of the PeNHX3 Protein

Transient expression assays (Figure 10) showed that the green fluorescence of PeNHX3-GFP outlined the cell periphery of tobacco mesophyll cells and completely overlapped with the mCherry membrane marker, indicating that PeNHX3 localizes to the plasma membrane rather than to the vacuolar membrane suggested by its phylogenetic placement.

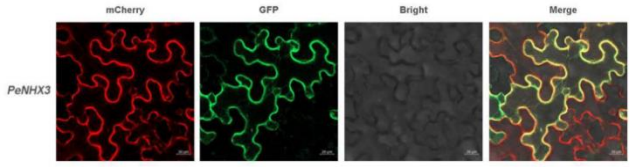


Figure 10. *Subcellular localization of PeNHX3 in Nicotiana benthamiana.*

3.9. Heterologous Overexpression of *PeNHX3* Enhances Salt Tolerance in Arabidopsis

3.9.1. Generation and Expression Analysis of Transgenic Lines

Multiple transgenic lines were obtained after kanamycin screening and PCR identification. qRT-PCR analysis showed that *PeNHX3* transcripts were significantly up-regulated in all lines, with OE-10 reaching approximately 37-fold and OE-8 and OE-12 reaching 26-fold and 27-fold of the wild-type level, respectively (Figure 11).

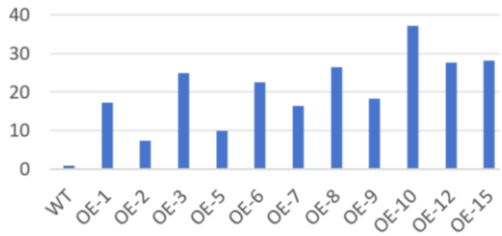


Figure 11. *Identification and expression analysis of PeNHX3-overexpression Arabidopsis lines.*

3.9.2. Growth Phenotypes of Transgenic Arabidopsis Under Salt Stress

Under 0 mmol/L NaCl, no phenotypic difference was observed between the wild type and the OE lines (Figure 12A). All lines were inhibited as the NaCl concentration increased, but the wild type suffered more severely: at 100 and 150 mmol/L NaCl, the wild type displayed shortened primary roots and chlorotic leaves, whereas the OE lines retained longer roots and green leaves.

3.9.3. Primary Root Length and Fresh Weight of Transgenic Arabidopsis Under Salt Stress

As shown in Figure 12B and Figure 12C, primary root length and fresh weight did not differ significantly among lines under normal conditions or 50 mmol/L NaCl; at 100 and 150 mmol/L NaCl, both parameters were significantly higher in the OE lines than in the wild type ($P<0.05$).

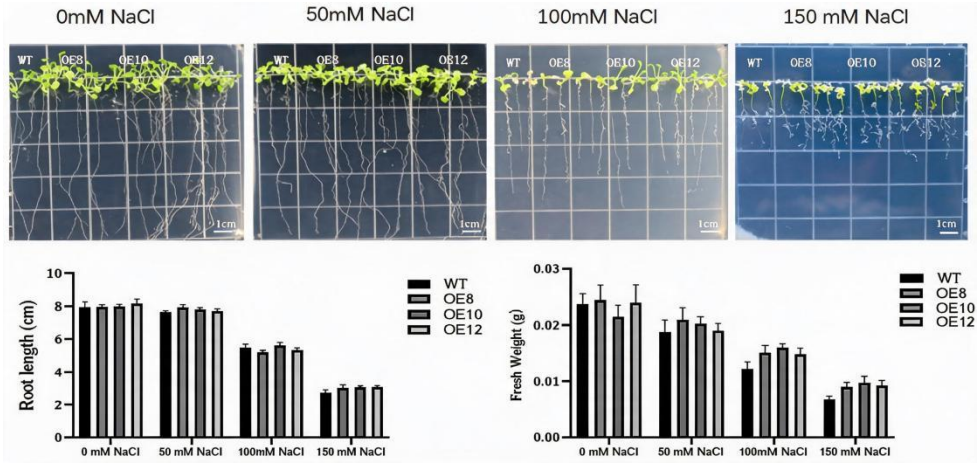


Figure 12. *Growth phenotypes (A), primary root length (B), and fresh weight (C) of PeNHX3-overexpression and wild-type Arabidopsis under salt stress.*

4. Discussion

In this study, six PeNHX members were identified, a number consistent with the report by Ye et al. [20]. However, *PeNHX6* deviates markedly from the other members in motif composition, isoelectric point, and phylogenetic position, indicating that functional divergence has occurred within this family; similar observations have been reported for the NHX family of rye [12].

ABRE was detected in the promoters of all six members, implying that ABA signaling participates in the transcriptional regulation of this family [27]. The presence of MBS, which is unique to *PeNHX4*, and of LTR in *PeNHX6* further suggests a division of roles among members in stress responses.

PeNHX3 was markedly up-regulated in roots, stems, and leaves, reaching approximately 33-fold of the control level in stems at 12 h. *P. euphratica* restricts Na^+ loading into leaves by sequestering Na^+ in xylem parenchyma cells of the stem [15]; the strong induction of *PeNHX3* in stems suggests that it participates in this process.

Phylogenetically, *PeNHX3* belongs to the Class I clade, yet it localized to the plasma membrane in our experiments. The C-terminal tail of NHX proteins participates in the control of targeting: *AtNHX1* loses its vacuolar targeting signal when the C terminus is deleted [25], and the construct used in this study carried a C-terminal GFP fusion, whose tag may interfere with targeting signals. In addition, *SOS1/NHX7* has been shown to localize not only to the plasma membrane for Na^+ efflux but also to late endosomes, where it participates in Na^+ sequestration [28]. Pan et al. [22] observed vacuolar membrane localization of *PeNHX3* in transgenic Arabidopsis, whereas the present study detected plasma membrane localization in *N. benthamiana*, suggesting that the membrane targeting of *PeNHX3* is influenced by the expression system and cell type [29].

Overexpression of *PeNHX3* increased primary root length and fresh weight under 100 and 150 mmol/L NaCl. In combination with its plasma membrane localization and strong induction in stems, we hypothesize that *PeNHX3* reduces cytosolic Na^+ load by promoting Na^+ efflux, an effect complementary to the Na^+ sequestration mediated by vacuolar NHXs [29].

This study has limitations: the transport selectivity and pH dependence of *PeNHX3* need to be determined by electrophysiological approaches; its localization needs to be confirmed with N-terminal fusion and C-terminal truncation constructs; and the transferred DNA (T-DNA) copy numbers of the transgenic lines as well as the Na^+ and K^+ contents of the plants have not yet been measured.

5. Conclusions

Six PeNHX family members were identified from the genome of *P. euphratica*. *PeNHX3* showed the strongest induction under salt stress (approximately 33-fold in stems at 12 h), and its protein product localizes to the plasma membrane. Overexpression of *PeNHX3* increased primary root length and fresh weight of Arabidopsis under salt stress; it is therefore a candidate gene for salt-tolerance breeding of woody plants.

Abbreviations

ABA	Abscisic Acid
ABRE	ABA-responsive Element
ARE	Anaerobic-Responsive Element
AtNHX	Arabidopsis Thaliana NHX
CDD	Conserved Domain Database
CPA1	Cation/Proton Antiporter 1
GFP	Green Fluorescent Protein
MBS	MYB Binding Site
MeJA	Methyl Jasmonate
MES	2-(N-morpholino)ethanesulfonic Acid
MS	Murashige and Skoog
MW	Molecular Weight
NHX	Na+/H+ Exchanger (antiporter)
PeNHX	Populus Euphratica NHX
ROS	Reactive Oxygen Species
SOS1	Salt Overly Sensitive 1
T-DNA	Transferred DNA
TAIR	The Arabidopsis Information Resource
35S	Cauliflower Mosaic Virus 35S Promoter

Author Contributions

Peiyang He is the sole author. The author read and approved the final manuscript.

Funding

This research was funded by the National Natural Science Foundation of China (grant number 32370377).

Data Availability Statement

All data supporting the conclusions are presented in this article; the genome sequences used are available at GWH (accession nos. GWHAAYU0000006.1, 0000007.1, 0000010.1, 0000013.1, 0000014.1)

Conflicts of Interest

The author declares no conflicts of interest.

References

[1] Wang, G. Z., Ni, G., Feng, G., et al. Saline-alkali soil reclamation and utilization in China: Progress and prospects. Frontiers of Agricultural Science and Engineering. 2024, 11(2), 216-228. https://doi.org/10.15302/J-FASE-2024551

[2] Yang, Y. Q., Guo, Y. Unraveling salt stress signaling in plants. Journal of Integrative Plant Biology. 2018, 60(9), 796-804. https://doi.org/10.1111/jipb.12689

[3] Van Zelm, E., Zhang, Y. X., Testerink, C. Salt tolerance mechanisms of plants. Annual Review of Plant Biology. 2020, 71, 403-433. https://doi.org/10.1146/annurev-arplant-050718-100005

[4] Zhu, J. K. Abiotic stress signaling and responses in plants. Cell. 2016, 167(2), 313-324. https://doi.org/10.1016/j.cell.2016.08.029

[5] Feng, K. Y., Zhao, X. Y., Li, Z. Y., et al. Research advances in the molecular mechanisms of plant response to saline-alkali stress. Biotechnology Bulletin. 2024, 40(10), 122-138. (in Chinese)https://doi.org/10.13560/j.cnki.biotech.bull.1985.2024-0410

[6] Bassil, E., Blumwald, E. The ins and outs of intracellular ion homeostasis: NHX-type cation/H^+ transporters. Current Opinion in Plant Biology. 2014, 22, 1-6. https://doi.org/10.1016/j.pbi.2014.08.002

[7] Apse, M. P., Aharon, G. S., Snedden, W. A., et al. Salt tolerance conferred by overexpression of a vacuolar Na^+/H^+ antiport in Arabidopsis. Science. 1999, 285(5431), 1256-1258. https://doi.org/10.1126/science.285.5431.1256

[8] Bassil, E., Ohto, M. A., Esumi, T., et al. The Arabidopsis intracellular Na^+/H^+ antiporters NHX5 and NHX6 are endosome associated and necessary for plant growth and development. The Plant Cell. 2011, 23(1), 224-239. https://doi.org/10.1105/tpc.110.079426

[9] Shi, H. Z., Lee, B. H., Wu, S. J., et al. Overexpression of a plasma membrane Na^+/H^+ antiporter gene improves salt tolerance in Arabidopsis thaliana. Nature Biotechnology. 2003, 21(1), 81-85. https://doi.org/10.1038/nbt766

[10] Sharma, P., Mishra, S., Pandey, B., et al. Genome-wide identification and expression analysis of the NHX gene family under salt stress in wheat (Triticum aestivum L.). Frontiers in Plant Science. 2023, 14, 1266699. https://doi.org/10.3389/fpls.2023.1266699

[11] Xie, F. Y., Chen, L. H., Cao, L. S., et al. Characterization of the NHX gene family in Tetragonia tetragonoides and its expression patterns under abiotic stresses. Guangdong Agricultural Sciences. 2025, 52(7), 104-117. (in Chinese) https://doi.org/10.16768/j.issn.1004-874X.2025.07.010

[12] Wang, Z. Y., Cui, Y. Y., Han, M. Q., et al. Identification and expression analysis of the NHX gene family under salt stress in rye. Acta Agriculturae Boreali-Sinica. 2025, 40(3), 9-18. (in Chinese)https://doi.org/10.7668/hbnxb.20195534

[13] Fukuda, A., Nakamura, A., Hara, N., et al. Molecular and functional analyses of rice NHX-type Na^+/H^+ antiporter genes. Planta. 2011, 233(1), 175-188. https://doi.org/10.1007/s00425-010-1289-4

[14] Huertas, R., Rubio, L., Cagnac, O., et al. The K^+/H^+ antiporter LeNHX2 increases salt tolerance by improving K^+ homeostasis in transgenic tomato. Plant, Cell and Environment. 2013, 36(12), 2135-2149. https://doi.org/10.1111/pce.12109

[15] Chen, S. L., Polle, A. Salinity tolerance of Populus. Plant Biology. 2010, 12(2), 317-333. https://doi.org/10.1111/j.1438-8677.2009.00301.x

[16] Ma, T., Wang, J. Y., Zhou, G. K., et al. Genomic insights into salt adaptation in a desert poplar. Nature Communications. 2013, 4, 2797. https://doi.org/10.1038/ncomms3797

[17] Ge, X. L., Zhang, L., Du, J. J., et al. Transcriptome analysis of Populus euphratica under salt treatment and PeERF1 gene enhances salt tolerance in transgenic Populus alba ×P. glandulosa. International Journal of Molecular Sciences. 2022, 23(7), 3727. https://doi.org/10.3390/ijms23073727

[18] Dai, X. R., Yang, Y. F., Ren, X. R., et al. Overexpression of Populus euphratica PeHINT2 enhances plant salt tolerance. Journal of Beijing Forestry University. 2025, 47(10), 96-107. (in Chinese)https://doi.org/10.12171/j.1000-1522.20250262

[19] Jia, H. X., Liu, G. J., Li, J. B., et al. Genome resequencing reveals demographic history and genetic architecture of seed salinity tolerance in Populus euphratica. Journal of Experimental Botany. 2020, 71(14), 4308-4320. https://doi.org/10.1093/jxb/eraa172

[20] Ye, C. Y., Zhang, H. C., Chen, J. H., et al. Molecular characterization of putative vacuolar NHX-type Na^+/H^+ exchanger genes from the salt-resistant tree Populus euphratica. Physiologia Plantarum. 2009, 137(2), 166-174. https://doi.org/10.1111/j.1399-3054.2009.01269.x

[21] Wang, L., Feng, X., Zhao, H., et al. Functional analysis of the Na^+, K^+/H^+ antiporter PeNHX3 from the tree halophyte Populus euphratica in yeast by model-guided mutagenesis. PLoS ONE. 2014, 9(8), e104147. https://doi.org/10.1371/journal.pone.0104147

[22] Pan, T., Liu, Y. F., Su, X. M., et al. Domain-switch analysis of PeNHX3 from Populus euphratica reveals the critical role of the transmembrane domain 11 in Na^+ and Li^+ transport. Journal of Plant Physiology. 2017, 219, 1-11. https://doi.org/10.1016/j.jplph.2017.09.003

[23] Livak, K. J., Schmittgen, T. D. Analysis of relative gene expression data using real-time quantitative PCR and the $2^{-\Delta\Delta Ct}$ method. Methods. 2001, 25(4), 402-408. https://doi.org/10.1006/meth.2001.1262

[24] Sparkes, I. A., Runions, J., Kearns, A., et al. Rapid, transient expression of fluorescent fusion proteins in tobacco plants and generation of stably transformed plants. Nature Protocols. 2006, 1(4), 2019-2025. https://doi.org/10.1038/nprot.2006.286

[25] Reguera, M., Bassil, E., Tajima, H., et al. pH regulation by NHX-type antiporters is required for receptor-mediated protein trafficking to the vacuole in Arabidopsis. The Plant Cell. 2015, 27(4), 1200-1217. https://doi.org/10.1105/tpc.114.135699

[26] Clough, S. J., Bent, A. F. Floral dip: a simplified method for Agrobacterium-mediated transformation of Arabidopsis thaliana. The Plant Journal. 1998, 16(6), 735-743. https://doi.org/10.1046/j.1365-313X.1998.00343.x

[27] Yoshida, T., Mogami, J., Yamaguchi-Shinozaki, K. ABA-dependent and ABA-independent signaling in response to osmotic stress in plants. Current Opinion in Plant Biology. 2014, 21, 133-139. https://doi.org/10.1016/j.pbi.2014.07.009

[28] Ramakrishna, P., Gámez-Arjona, F. M., Bellani, E., et al. Elemental cryo-imaging reveals SOS1-dependent vacuolar sodium accumulation. Nature. 2025, 637(8048), 1228-1233. https://doi.org/10.1038/s41586-024-08403-y

[29] Abdelrady, W. A., Mostafa, K., Saeed, M., et al. NHX transporters: molecular mechanisms and applications for enhancing crop resilience to soil salinity in changing environments. Plant Physiology and Biochemistry. 2025, 229, 110603. https://doi.org/10.1016/j.plaphy.2025.110603